

1 **Triple oxygen isotopes indicate urbanization affects sources of**
2 **nitrate in wet and dry atmospheric deposition**

3
4
5
6 David M. Nelson^{1,2}, Urumu Tsunogai², Ding Dong², Takuya Ohyama², Daisuke D. Komatsu^{2,†},
7 Fumiko Nakagawa², Izumi Noguchi³, Takashi Yamaguchi³

8
9
10
11 ¹ University of Maryland Center for Environmental Science, Appalachian Laboratory, Frostburg, MD, 21532, USA

12 ² Nagoya University, Graduate School of Environmental Studies, Nagoya, 464-8601, Japan

13 ³ Hokkaido Research Organization, Department of Environmental and Geological Research, Institute of
14 Environmental Sciences, Sapporo, 060-0819, Japan

15
16
17
18
19
20
21
22 *Correspondence to:* David M. Nelson (dnelson@umces.edu)

23 [†]Present address: Tokai University, Department of Marine and Earth Science

24 **Abstract**

25 Atmospheric nitrate deposition resulting from anthropogenic activities negatively affects human and
26 environmental health. Identifying deposited nitrate that is produced locally vs. that originating from long-distance
27 transport would help inform efforts to mitigate such impacts. However, distinguishing the relative transport
28 distances of atmospheric nitrate in urban areas remains a major challenge since it may be produced locally and/or
29 come from upwind regions. To address this uncertainty we assessed spatiotemporal variation in monthly
30 weighted-average $\Delta^{17}\text{O}$ and $\delta^{15}\text{N}$ values of wet and dry nitrate deposition during one year at urban and rural sites
31 along the western coast of the northern Japanese island of Hokkaido, downwind of the East Asian continent. $\Delta^{17}\text{O}$
32 values of nitrate in wet deposition at the urban site mirrored those of wet and dry deposition at the rural site, ranging
33 between $\sim +23$ and $+31$ ‰ with higher values during winter and lower values in summer, which suggests greater
34 relative importance of oxidation of NO_2 by O_3 during winter and OH during summer. In contrast, $\Delta^{17}\text{O}$ values of
35 nitrate in dry deposition at the urban site were lower ($+19$ - $+25$ ‰) and displayed less distinct seasonal variation.
36 Furthermore, the difference between $\delta^{15}\text{N}$ values of nitrate in wet and dry nitrate deposition was, on average, 3 ‰
37 greater at the urban than rural site, and $\Delta^{17}\text{O}$ and $\delta^{15}\text{N}$ values were correlated for both forms of deposition at both
38 sites with the exception of dry deposition at the urban site. These results suggest that, relative to nitrate in wet and
39 dry deposition in rural environments and wet deposition in urban environments, nitrate in dry deposition in urban
40 environments forms from relatively greater oxidation of NO by peroxy radicals and/or oxidation of NO_2 by OH .
41 Given greater concentrations of peroxy radicals and OH in cities, these results imply that dry nitrate deposition
42 results from local NO_x emissions more so than wet deposition, which is transported longer distances. These results
43 illustrate the value of stable isotope data for distinguishing the transport distances and reaction pathways of
44 atmospheric nitrate pollution.

45

46

47

48 **1 Introduction**

49 The world's urban population has rapidly grown in recent decades, and this trend is expected to continue
50 for at least a generation (United Nations, 2014). Besides socioeconomic transformation, urbanization also has
51 environmental consequences, such as air pollution (Bloom et al., 2008; Cumming et al., 2014; Akimoto, 2003;
52 Gurjar et al., 2016; von Glasow et al., 2013). For example, fossil fuel combustion from mobile and stationary
53 sources produces nitrogen oxides ($\text{NO}_x = \text{NO} + \text{NO}_2$), which mediate atmospheric ozone (O_3) and fine-particle
54 production, thus affecting human health. Furthermore, oxidation of NO_x leads to the formation of nitrate (NO_3^-),
55 which when deposited on Earth's surface contributes to the acidification and eutrophication of ecosystems
56 (Galloway et al., 2004; Brown et al., 2006; Crutzen, 1979). Efforts to reduce NO_x emissions can mitigate nitrate
57 deposition (Liu et al., 2016; Zhao et al., 2015), but NO_x and atmospheric nitrate are also transported long distances
58 and thus can affect areas far downwind of production hotspots (Holtgrieve et al., 2011; Akimoto, 2003; Lin et al.,
59 2017). The pathways that transform NO_x to nitrate (Figure 1), as well as the spatiotemporal patterns of atmospheric
60 nitrate deposition, are relatively well understood (Ban et al., 2016; Li et al., 2016). However, it remains challenging
61 to identify the sources of many pollutants, including nitrate produced locally vs. originating from long-distance
62 transport, which impedes efforts to improve air quality and environmental conditions (Wagstrom and Pandis, 2011;
63 Skyllakou et al., 2014).

64 The stable nitrogen and oxygen isotope compositions of nitrate have been suggested as potential tracers of
65 the sources and fate of NO_x in the environment (Elliott et al., 2009; Kendall et al., 2007; Freyer et al., 1993).
66 Nitrogen isotopes ($\delta^{15}\text{N}$) of nitrate can potentially reflect those of NO_x , but mass-dependent isotopic fractionations
67 during the oxidation of NO_x to nitrate can also alter the original $\delta^{15}\text{N}$ value of NO_x , thus complicating efforts to use
68 $\delta^{15}\text{N}$ values of nitrate for source partitioning (e.g. Walters and Michalski, 2015, 2016; Walters et al., 2016). A

69 unique alternative that has recently emerged is the triple oxygen isotope ($\Delta^{17}\text{O}$) value of nitrate¹, which reflects (as
70 the result of mass-independent isotopic fractionation during the formation of O_3) the number of oxygen atoms
71 derived from O_3 that are involved in the oxidation of NO_x (Alexander et al., 2009; Morin et al., 2008; Michalski et
72 al., 2003; Tsunogai et al., 2010; Tsunogai et al., 2016) since direct emissions of nitrate during combustion are
73 relatively small (Fraser et al., 1998). An advantage of $\Delta^{17}\text{O}$ relative to $\delta^{18}\text{O}$ of nitrate is that $\Delta^{17}\text{O}$ values are
74 primarily a function of the chemical pathways of nitrate formation, whereas $\delta^{18}\text{O}$ values are also influenced by $\delta^{18}\text{O}$
75 of atmospheric water and temperature (Michalski et al., 2011). The fraction of NO oxidized to NO_2 by O_3 relative to
76 peroxy radicals ($\text{HO}_2 + \text{RO}_2$) determines two-thirds of the $\Delta^{17}\text{O}$ value of nitrate. The remaining fraction results from
77 the extent to which O_3 vs. OH molecules oxidize NO_2 (Geng et al., 2017). $\Delta^{17}\text{O}$ values of atmospheric nitrate
78 deposition are often highest in winter and lowest in summer (Michalski et al., 2003; Savarino et al., 2007; Tsunogai
79 et al., 2010; Tsunogai et al., 2016), because greater darkness and lower temperatures favor the oxidation of NO_x by
80 O_3 , as well as N_2O_5 hydrolysis reactions, whereas oxidation of NO_2 by OH is more important when daylight is
81 longer and temperatures higher (Figure 1). Peroxy radicals, which form from oxidation of carbon monoxide, reactive
82 hydrocarbons, and volatile organic compounds (Saito et al., 2002), are thought to compete with O_3 to oxidize NO in
83 polluted settings and thus depress $\Delta^{17}\text{O}$ values of nitrate (Guha et al., 2017; Fang et al., 2011). Decreasing
84 nitrate- $\Delta^{17}\text{O}$ values during the past ~150 years in West Antarctica suggest that anthropogenic activities have
85 increased the relative importance of peroxy radicals in NO_x cycling globally (Sofen et al., 2014). However, reactive
86 hydrocarbons and aerosols can also facilitate the formation of nitrate directly or through N_2O_5 , respectively, which
87 elevates $\Delta^{17}\text{O}$ values of nitrate (Michalski et al., 2011). Although wet (aqueous nitrate) and dry (gaseous HNO_3 or

¹ $\Delta^{17}\text{O}$ values are defined as:
$$\Delta^{17}\text{O}_{\text{nitrate}} = \frac{1 + \delta^{17}\text{O}_{\text{nitrate}}}{\left(1 + \delta^{18}\text{O}_{\text{nitrate}}\right)^\beta} - 1$$

where $\beta = 0.5279^{18}$, $\delta = [\text{R}_{\text{sample}}/\text{R}_{\text{standard}}] - 1$, and R represents the elemental ratios (i.e., $^{17}\text{O}/^{16}\text{O}$ and $^{18}\text{O}/^{16}\text{O}$) between a sample and standard.

88 particulate nitrate) deposited nitrate are often presumed to have similar $\Delta^{17}\text{O}$ values (Guerrieri et al., 2015), dry
89 deposition may be less prone to long-distance transport (Celle-Jeanton et al., 2009; Dasch and Cadle, 1985;
90 Balestrini et al., 2000). Shorter transport distances could lead to distinct oxidation pathways and thus different $\Delta^{17}\text{O}$
91 values of nitrate between these forms of deposition in urban environments where concentrations of atmospheric
92 pollutants are typically elevated. Yet, this hypothesis cannot be evaluated using existing data, as prior studies
93 typically analyzed $\Delta^{17}\text{O}$ values of only wet or dry nitrate deposition at single sites (Guha et al., 2017; Tsunogai et al.,
94 2010).

95 Here we assess the effect of urbanization on the oxidation chemistry of NO_x and the sources of nitrate in
96 wet and dry atmospheric deposition using measurements of the $\Delta^{17}\text{O}$, $\delta^{18}\text{O}$, and $\delta^{15}\text{N}$ values of nitrate. Our two study
97 sites (Figure 2) are located at a similar longitude, are separated by only $\sim 2^\circ$ of latitude, and have comparable
98 synoptic climatologies, but there is a major difference in the degree of urbanization between them (see below).
99 These sites were chosen to be downwind of several megacities on the East Asian continent, a region where NO_x
100 emissions have increased approximately four-fold during the past forty years (Akimoto, 2003; Uno et al., 2007).
101 This arrangement of sites provides an ideal setting to investigate potential differences in the oxidation pathways and
102 sources of nitrate pollution in urban and rural environments against high background levels of atmospheric nitrate
103 deposition.

104

105 **2 Material and Methods**

106 **2.1 Study sites**

107 Rishiri is a remote (population size: $\sim 5,000$; density: ~ 28 people/ km^2) and small island in the Sea of Japan
108 off the coast of the island of Hokkaido in northern Japan. Samples of wet and dry atmospheric deposition were
109 collected at the Rishiri National Acid Rain Monitoring station (Figure 2; $45^\circ 07' 11''$ N, $141^\circ 12' 33''$ E; 40 m a.s.l.),
110 which is part of the Acid Deposition Monitoring Network in East Asia (EANET), between January and December in
111 2009. The mean annual precipitation is ~ 920 mm and mean annual temperature is $\sim 7.1^\circ\text{C}$

112 (<http://www.jma.go.jp/jma/indexe.html>). Precipitation amounts are the highest in the late summer through winter,
113 with lower amounts in the spring and early summer. The main land cover within a ~10 km radius of the monitoring
114 station is forest and shrub land.

115 Sapporo is a city of ~1.9 million people (density: ~1,710 people/km²) that is ~200 km south of Rishiri.
116 Samples of wet and dry atmospheric deposition were obtained from the roof of the Institute of Environmental
117 Sciences in Sapporo (Figure 2; 43° 04' 55" N, 141° 20' 00" E; ~26 m a.s.l.) between January and December in 2009.
118 The sampling site in Sapporo is not part of EANET. The mean annual precipitation is ~1,100 mm and mean annual
119 temperature is ~8.9°C (<http://www.jma.go.jp/jma/indexe.html>). Rishiri and Sapporo are both located on the Sea of
120 Japan side of Hokkaido prefecture and thus they have similar seasonal precipitation patterns and air-mass
121 back-trajectories on daily and longer time scales. Sapporo is bordered by the Sea of Japan to the north and by
122 mountains to the west, south, and east. The major sources of local NO_x emissions are automobile exhaust and boilers
123 used for domestic heating. There are no major factories or combustion-based electricity generation facilities in
124 Sapporo (Kaneyasu et al., 1995). The prevailing winds in Hokkaido typically originate from the northwest in winter
125 and southeast in summer (Kaneyasu et al., 1995).

126 **2.2 Sample collection**

127 Samples were collected using the standard operating methods of EANET
128 (<http://www.eanet.asia/product/manual/techacm.pdf>). Composite samples of wet deposition falling on a daily and
129 weekly basis were collected at Rishiri (n= 62) and Sapporo (n = 41), respectively, using auto samplers (DKK
130 DRS-200(S), DKK and US-420, Ogasawara Keiki Corp, respectively). The wet deposition samples were filtered
131 through a 0.45 µm filter and stored at 4°C until measurement of nitrate and nitrite (NO₂⁻) concentrations and
132 isotopes.

133 Samples of dry deposition were obtained using the filter-pack method, which has been widely used in dry
134 deposition monitoring programs throughout the world (Aikawa et al., 2010; Endo et al., 2011; Mehlmann and
135 Warneck, 1995; Tørseth et al., 1999). At each site, air was drawn through a four-stage filter pack at a rate of 4 L/min

136 to collect gaseous HNO₃ and particulate nitrate. Composite samples collected using this approach (which we refer to
137 as dry deposition) were obtained on a monthly basis at Rishiri (n = 12). Sampling of dry deposition at Sapporo
138 occurred approximately bi-weekly (n = 24); sampling occurred bi-weekly rather than monthly (as at Rishiri) because
139 we anticipated higher nitrate concentrations in dry deposition at Sapporo than Rishiri. However, only 15 of the 24
140 dry deposition samples from Sapporo were available for analysis in the present study. The first stage of the filter
141 pack is a multi-nozzle cascade impactor (NL-4-10P, Tokyo Dylec. Corp.) and Teflon binder filter (T60A20-20H,
142 Tokyo Dylec. Corp.) that collects coarse particles >10 μm in diameter. The second stage is a Teflon filter
143 (ADVANTEC T080A047A) that collects fine particles <10 μm in diameter that passed through the first filter. The
144 third stage is a 0.45 μm nylon filter (PALL ULTIPOR N66-NX047100) that collects HNO₃ gas and some SO₂, HCl,
145 HONO, NH₃, and NO₂. The 4th and 5th stage filters (ADVANTEC No. 51A, alkaline impregnated filter) are used to
146 collect the remaining SO₂, HCl, and HONO. The last filter (ADVANTEC No. 51A, acid impregnated filter) is used
147 to collect the remaining NH₃. The nitrate and nitrite on the first, second, and third filters were extracted using
148 ultrapure water, passed through a 0.45 μm filter, and stored at 4°C until measurement of nitrate and nitrite
149 concentrations and isotopes.

150 The maximum filter blank was 0.2 μg (=3 nmol) for nitrate, which corresponds to 0.16 μmol/L nitrate
151 when 20 mL of milli-Q water is used to extract nitrate from each filter based on the EANET procedure. The
152 minimum nitrate concentrations in the solutions extracted from the filters and measured for isotopic values were
153 30.7 μmol/L, 1.5 μmol/L, and 22.4 μmol/L in the portions of coarse particles, fine particles, and gas, respectively,
154 for Rishiri, and 26.1 μmol/L, 3.5 μmol/L, and 10.2 μmol/L in the portions of coarse particles, fine particles, and gas,
155 respectively, for Sapporo. Thus, we concluded that the blanks had little influence on the isotopic values of dry
156 deposition. This is true even for fine particle samples with nitrate concentrations <5 μmol/L, because the deposition
157 rates of these nitrate-depleted samples were low. We did not directly assess filter breakthrough limits, but prior
158 results based on changes in the duration of sampling at our sites suggest that such limits are much higher than the
159 amount of nitrate present in our samples (Noguchi et al., 2009).

160 2.3 Analysis

161 Within a few months of collection, nitrate and nitrite in the filtered samples of wet and dry deposition
162 were quantified using ion chromatography (Dionex DX-500, ICS-1500 and ICS-2000, Nippon Dionex Co., Ltd.,
163 Osaka, Japan). Based on replicate analyses of samples, the precision of these concentration measurements was 1.6 %.
164 The detection limit was 0.03 $\mu\text{mol/L}$. Nitrite concentrations were < 1.0 % of the sum of nitrite and nitrate
165 concentrations in all samples of wet deposition, and they were ≤ 5.0 % in 72 % and 87 % of samples of dry
166 deposition at Rishiri and Sapporo, respectively. The pH values of the wet deposition samples ranged between 4.51
167 and 5.02 at Rishiri and between 4.65 and 5.29 at Sapporo.

168 Isotopic analysis was performed in 2013 for samples from Rishiri and in 2011 for samples from Sapporo.
169 Prior to isotopic analysis we reanalyzed nitrate and nitrate concentrations in the samples and found that differences
170 between these and the original concentration measurements were < 10 %. For isotopic analysis, nitrite and nitrate in
171 each filtrate sample was converted to N_2O using chemical conversion (McIlvin and Altabet, 2005) with slight
172 modification (Tsunogai et al., 2016; Tsunogai et al., 2008). Isotopic analysis of nitrite alone was also performed on
173 samples with nitrite concentrations > 5.0 % of the total nitrite plus nitrate concentrations (McIlvin and Altabet,
174 2005). The $\delta^{15}\text{N}$, $\delta^{18}\text{O}$, and $\Delta^{17}\text{O}$ values of N_2O in each vial were determined using a continuous-flow isotope ratio
175 mass spectrometry system (Komatsu et al., 2008; Hirota et al., 2010). The obtained $\delta^{18}\text{O}$ values were normalized to
176 VSMOW using local laboratory nitrate standards calibrated against USGS 34 ($\delta^{18}\text{O} = -27.9$ ‰, $\Delta^{17}\text{O} = 0.04$ ‰, and
177 $\delta^{15}\text{N} = -1.8$ ‰) and USGS 35 ($\delta^{18}\text{O} = +57.5$ ‰, $\Delta^{17}\text{O} = +20.88$ ‰, and $\delta^{15}\text{N} = +2.7$ ‰) (Kaiser et al., 2007). $\Delta^{17}\text{O}$
178 values were measured directly from the δ^{33} and δ^{34} of O_2 data. The obtained $\delta^{15}\text{N}$ values were normalized to Air
179 using local laboratory nitrate standards calibrated against USGS 32 ($\delta^{18}\text{O} = +25.7$ ‰ and $\delta^{15}\text{N} = +180$ ‰) and
180 USGS 34. The $\delta^{18}\text{O}$ and $\delta^{15}\text{N}$ values of the three local standards range between 1.1 and 22.4 ‰ and between -2.1
181 and 11.8 ‰, respectively. The $\Delta^{17}\text{O}$ values of the local standards are ~ 0 ‰. Analytical precision (1σ) was ± 0.3 ‰
182 for $\delta^{15}\text{N}$, ± 0.5 ‰ for $\delta^{18}\text{O}$, and ± 0.2 ‰ for $\Delta^{17}\text{O}$ based on repeated measurements of the local nitrate standards
183 (Tsunogai et al., 2010). Besides using the local nitrate standards for routine calibration and as checks of isotopic

184 fractionation and oxygen isotope exchanges, we also analyzed USGS34 and USGS 35 at least monthly to assess
185 instrument linearity.

186 For samples with nitrite concentrations $\geq 5\%$ of the total nitrite plus nitrate concentrations the $\delta^{15}\text{N}$ and
187 $\delta^{18}\text{O}$ values of nitrate were calculated by mass balance (e.g. $\delta^{15}\text{N}_{\text{NO}_3^-} = (\delta^{15}\text{N}_{\text{NO}_2^- + \text{NO}_3^-} * [\text{NO}_2^- + \text{NO}_3^-] - \delta^{15}\text{N}_{\text{NO}_2^-} * [\text{NO}_2^-]) / [\text{NO}_3^-]$). The measured $\Delta^{17}\text{O}$ value of nitrite for samples on which this analysis was performed was 0 ‰.
188 Therefore, we presumed that the $\Delta^{17}\text{O}$ value of nitrite is 0 ‰ because of rapid oxygen change between NO_2 and
189 water at near-neutral pH condition (Casciotti et al., 2007), and we corrected the $\Delta^{17}\text{O}$ values of nitrate as $\Delta^{17}\text{O}_{\text{NO}_3^-} =$
190 $\Delta^{17}\text{O}_{\text{NO}_2^- + \text{NO}_3^-} * [\text{NO}_2^- + \text{NO}_3^-] / [\text{NO}_3^-]$. For all samples (at both sites), the maximum nitrite/nitrate ratios in the
191 samples were 28.6, 13.3, and 7.4 % for coarse particles, fine particles, and gas, respectively. Therefore, the
192 maximum extent of $\delta^{15}\text{N}$ corrections for the limited number of dry deposition samples with nitrite concentrations > 5
193 % of the total nitrite plus nitrate concentrations were 1.1, 0.9 and < 0.1 ‰, respectively, the maximum extent of $\delta^{18}\text{O}$
194 corrections were 15.0, 11.2, and < 0.1 ‰, respectively, and the maximum extent of $\Delta^{17}\text{O}$ corrections were 5.7, 3.1,
195 and 0.4 ‰, respectively. From these results we conclude that the potential bias in the isotopic values of dry
196 deposition associated with nitrite was much smaller than the errors assumed in the final total isotopic values of dry
197 deposition (around ± 2.5 ‰ for $\delta^{15}\text{N}$, ± 8.0 ‰ for $\delta^{18}\text{O}$, and ± 3 ‰ for $\Delta^{17}\text{O}$).

198 To quantify the $\Delta^{17}\text{O}$, $\delta^{18}\text{O}$, and $\delta^{15}\text{N}$ values of nitrate in dry deposition, we calculated monthly
199 weighted-average (weighted based on mass) $\Delta^{17}\text{O}$, $\delta^{18}\text{O}$, and $\delta^{15}\text{N}$ values of nitrate (e.g. $\Delta^{17}\text{O}_{\text{dry}}$ and $\delta^{15}\text{N}_{\text{dry}}$,
200 respectively) among coarse and fine particles and gas phases using each isotopic value and concentration. For
201 Sapporo, isotopic values for samples of dry deposition collected during the same month were averaged as monthly
202 weighted-average values. To compare isotopic values of wet and dry deposition within and between sites, we
203 calculated monthly weighted-average $\Delta^{17}\text{O}$, $\delta^{18}\text{O}$ and $\delta^{15}\text{N}$ values of nitrate for wet deposition (e.g. $\Delta^{17}\text{O}_{\text{wet}}$ and
204 $\delta^{15}\text{N}_{\text{wet}}$). Paired t-tests were used to compare monthly weighted-average $\Delta^{17}\text{O}_{\text{wet}}$ and $\Delta^{17}\text{O}_{\text{dry}}$, $\delta^{18}\text{O}_{\text{wet}}$ and $\delta^{18}\text{O}_{\text{dry}}$, and
205 $\delta^{15}\text{N}_{\text{wet}}$ and $\delta^{15}\text{N}_{\text{dry}}$, within sites. Paired t-tests were also used to compare monthly weighted-average $\Delta^{17}\text{O}_{\text{coarse}}$ and
206 $\Delta^{17}\text{O}_{\text{fine}}$, $\delta^{18}\text{O}_{\text{coarse}}$ and $\delta^{18}\text{O}_{\text{fine}}$, and $\delta^{15}\text{N}_{\text{coarse}}$ and $\delta^{15}\text{N}_{\text{fine}}$ at each site. A one-way ANOVA was used to compare

208 monthly weighted-average $\Delta^{17}\text{O}_{\text{wet}}$ and $\Delta^{17}\text{O}_{\text{dry}}$ at Rishiri with $\Delta^{17}\text{O}_{\text{wet}}$ at Sapporo, as well as $\delta^{15}\text{N}_{\text{wet}}$ and $\delta^{15}\text{N}_{\text{dry}}$ at
209 Rishiri with $\delta^{15}\text{N}_{\text{wet}}$ at Sapporo. Statistical analyses were performed in PAST version 3.01 (Hammer et al., 2001).
210 Volatilization of particulate to gaseous nitrate that occurs using the filter-pack method (e.g. Noguchi et al., 2009)
211 may bias assessment of the isotopic values of gaseous and particulate nitrate. Therefore, we do not compare the
212 concentrations and isotopic values of particulate and gaseous nitrate at our sites.

213 Wet deposition flux was calculated using precipitation amount and nitrate concentration data obtained for
214 each site from the National Institute for Environmental Studies, Japan (<http://www.nies.go.jp/index-e.html>). The
215 monthly flux is the sum of precipitation amount multiplied by nitrate concentration for all samples in each month.

216 Dry deposition flux was estimated following the inferential method (Hicks, 1986), where

$$217 \quad F_{\text{dry}} = V_{\text{d}} \times C$$

218 and F_{dry} represents the dry deposition flux, V_{d} the deposition velocity, and C the nitrate concentration in air
219 (calculated from measured nitrate concentrations in the sample extracts and pumped air volume). Calculation of V_{d}
220 by the inferential method requires meteorological and land use data. Meteorological data were obtained from the
221 Japan Meteorological Agency (<http://www.jma.go.jp/jma/indexe.html>). Landuse was presumed to be forest at
222 Rishiri and city at Sapporo. The height of the forest canopy at Rishiri was presumed to be 10 m, and seasonal
223 canopy resistance was determined from NDVI values (Noguchi et al., 2006). Deposition velocity was calculated
224 using the inferential method version 4.2 (Noguchi et al., 2011; Wesely, 1989; Walcek et al., 1986; Erisman et al.,
225 1997; Zhang et al., 2003) (the program file is available at
226 http://www.hro.or.jp/list/environmental/research/ies/katsudo/acid_rain/kanseichinchaku/dry_deposition.html).
227 Deposition velocities of gaseous and particulate materials are estimated separately, although these results should be
228 interpreted with caution because of the potential for bias from volatilization of particulate nitrate. Fluxes of coarse
229 and fine particles were not differentiated.

230

231 **3 Results**

232 At the rural site, Rishiri, there was no difference between monthly weighted-average $\Delta^{17}\text{O}_{\text{dry}}$ and $\Delta^{17}\text{O}_{\text{wet}}$,
233 which ranged between +22.3 and +30.1 ‰ and between +22.7 and +30.3 ‰, respectively (Figure 3; $p = 0.57$, $n =$
234 12). Monthly weighted-average $\delta^{18}\text{O}_{\text{dry}}$ was overall slightly less than $\delta^{18}\text{O}_{\text{wet}}$, with ranges between +66.9 and
235 +94.4 ‰ and +71.2 and +90.9 ‰, respectively (Figure 3; $p = 0.005$, $n = 12$). Both forms of deposition exhibited
236 generally larger $\Delta^{17}\text{O}$ and $\delta^{18}\text{O}$ values in the winter than summer (Figures 3 and 4). $\Delta^{17}\text{O}_{\text{coarse}}$ was more positive (by
237 4.2 ‰, on average) than $\Delta^{17}\text{O}_{\text{fine}}$ ($p = 0.002$, $n = 10$) and $\delta^{18}\text{O}_{\text{coarse}}$ was more positive (by 4.6 ‰, on average) than
238 $\delta^{18}\text{O}_{\text{fine}}$ ($p = 0.01$, $n = 12$; Figure S1). Monthly weighted-average $\delta^{15}\text{N}_{\text{dry}}$ at Rishiri varied between -4.8 and +7.5 ‰
239 and was on average 3.5 ‰ larger than $\delta^{15}\text{N}_{\text{wet}}$, which varied between -8.6 and +2.0 ‰ (Figure 3; $p = 0.02$, $n = 12$).
240 $\delta^{15}\text{N}_{\text{coarse}}$ was slightly lower than $\delta^{15}\text{N}_{\text{fine}}$ at Rishiri ($p = 0.06$, $n = 10$).

241 At the urban site, Sapporo, monthly weighted-average $\Delta^{17}\text{O}_{\text{wet}}$ ranged between +23.0 and +30.8 ‰ and was
242 higher than $\Delta^{17}\text{O}_{\text{dry}}$, which ranged between +18.8 and +25.0 ‰ ($p < 0.001$, $n = 12$; Figure 3). Monthly
243 weighted-average $\delta^{18}\text{O}_{\text{wet}}$ was higher than $\delta^{18}\text{O}_{\text{dry}}$, with ranges between +70.7 and +92.2 ‰ and +56.8 and +70.8 ‰,
244 respectively (Figure 3; $p < 0.0001$, $n = 12$). $\Delta^{17}\text{O}_{\text{dry}}$ and $\delta^{18}\text{O}_{\text{dry}}$ at Sapporo displayed less pronounced seasonal
245 variation than $\Delta^{17}\text{O}_{\text{wet}}$ and $\delta^{18}\text{O}_{\text{wet}}$ (Figures 3 and 4). $\Delta^{17}\text{O}_{\text{coarse}}$ was more positive (by 3.9 ‰, on average) than
246 $\Delta^{17}\text{O}_{\text{fine}}$ ($p < 0.001$, $n = 12$) and $\delta^{18}\text{O}_{\text{coarse}}$ was more positive (by 7.3 ‰, on average) than $\delta^{18}\text{O}_{\text{fine}}$ (and $p = 0.004$, $n =$
247 12, respectively) at Sapporo (Figure S1). Monthly weighted-average $\delta^{15}\text{N}_{\text{dry}}$ at Sapporo varied between +0.5 and
248 +11.2 ‰ and was on average 6.5 ‰ larger than $\delta^{15}\text{N}_{\text{wet}}$, which varied between -4.7 and +3.4 ‰ (Figure 3; $p < 0.001$,
249 $n = 12$). $\delta^{15}\text{N}_{\text{coarse}}$ was on average 3.4 ‰ less than $\delta^{15}\text{N}_{\text{fine}}$ at Sapporo ($p = 0.04$, $n = 12$).

250 $\Delta^{17}\text{O}_{\text{wet}}$ at Sapporo exhibited similar values and seasonal patterns as $\Delta^{17}\text{O}_{\text{dry}}$ and $\Delta^{17}\text{O}_{\text{wet}}$ at Rishiri ($p = 0.97$,
251 $n = 12$). The difference between $\delta^{15}\text{N}_{\text{dry}}$ and $\delta^{15}\text{N}_{\text{wet}}$ was greater at Sapporo than Rishiri, and thus $\delta^{15}\text{N}_{\text{dry}}$ was greater
252 at Sapporo than Rishiri despite $\delta^{15}\text{N}_{\text{wet}}$ at Sapporo having similar values and seasonal patterns as $\delta^{15}\text{N}_{\text{wet}}$ ($p = 0.36$, n
253 $= 12$) and $\delta^{15}\text{N}_{\text{dry}}$ ($p = 0.46$, $n = 12$) at Rishiri (Figures 3 and 4). There were positive correlations between the $\delta^{15}\text{N}$
254 and $\Delta^{17}\text{O}$ values of wet and dry deposition at both sites, with the exception of dry deposition at Sapporo (Figure 5).
255 Fluxes of nitrate in dry particulate deposition and gaseous dry deposition were generally greater at Sapporo than

256 Rishiri (Figure S1) because the dry deposition velocity dominates the flux value of dry deposition and it is greater
257 for Rishiri (assumed to be forest) than Sapporo (assumed to be urban).

258

259 **4 Discussion**

260 The similar values and seasonal trends of $\Delta^{17}\text{O}_{\text{dry}}$ and $\Delta^{17}\text{O}_{\text{wet}}$ at Rishiri imply that both forms of
261 deposition experienced similar seasonal variation in photochemical reactions during their production from NO_x . The
262 values and trends are consistent with prior empirical studies of $\Delta^{17}\text{O}_{\text{wet}}$ at Rishiri between 2006 and 2007 (Tsunogai
263 et al., 2010) and elsewhere in Japan (Tsunogai et al., 2016). These results also coincide well with model predictions
264 (Alexander et al., 2009), which suggest that they indicate seasonal variation in the relative importance of oxidation
265 of NO_2 by O_3 vs. OH in background, free tropospheric air. During summer when solar radiation is high, the relative
266 importance of oxidation of NO_2 by OH is likely greatest, thus decreasing nitrate $\Delta^{17}\text{O}$ values. In contrast, solar
267 radiation is low in winter, which likely causes pathways involving oxidation of NO_2 by O_3 to be relatively more
268 important, thus increasing nitrate $\Delta^{17}\text{O}$ values. Values of $\Delta^{17}\text{O}_{\text{wet}}$ at Sapporo were indistinct from those of $\Delta^{17}\text{O}_{\text{dry}}$
269 and $\Delta^{17}\text{O}_{\text{wet}}$ at Rishiri, and the most straightforward interpretation of these results is that wet deposition at Sapporo
270 underwent similar photochemical formation processes as both forms of deposition at Rishiri.

271 In contrast to $\Delta^{17}\text{O}_{\text{dry}}$ and $\Delta^{17}\text{O}_{\text{wet}}$ at Rishiri and $\Delta^{17}\text{O}_{\text{wet}}$ at Sapporo, values of $\Delta^{17}\text{O}_{\text{dry}}$ at Sapporo were
272 lower and displayed less seasonal variation. These results suggest unique oxidation processes that display little
273 seasonal variation and are associated with dry deposition at this site. One potential explanation for the relatively low
274 $\Delta^{17}\text{O}_{\text{dry}}$ values at Sapporo relates to OH. Concentrations of OH are typically higher in urban than rural areas as the
275 result of the formation of OH from Criegee intermediates during alkene oxidation and/or photolysis of nitrous acid
276 or formaldehyde in more polluted urban settings (Monks, 2005). OH competes with O_3 to oxidize NO_2 , and thus
277 greater oxidation of NO_2 by OH in dry deposition would drive down $\Delta^{17}\text{O}_{\text{dry}}$ values (Morin et al., 2011). Another
278 potential explanation for the relatively low $\Delta^{17}\text{O}_{\text{dry}}$ at Sapporo relates to peroxy radicals potentially being of greater
279 importance in the oxidation of NO to NO_2 in dry deposition at this site. Peroxy radicals typically form via

280 photochemical oxidation of non-methane hydrocarbons that originate from anthropogenic sources, such as vehicle
281 exhaust, and their concentrations are usually higher in urban than rural environments (Saito et al., 2002; Carslaw et
282 al., 2002). These radicals rapidly compete with O₃ to oxidize NO to NO₂ (Monks, 2005), which results in lower
283 $\Delta^{17}\text{O}_{\text{dry}}$ values (Morin et al., 2011). A recent study also suggested that formation of NO₂ by reaction of peroxy
284 radicals with NO in polluted air caused short-term shifts toward lower $\Delta^{17}\text{O}_{\text{dry}}$ in Taiwan (Guha et al., 2017).
285 Atmospheric inversions are common in Sapporo (Uno et al., 1988) and other Japanese cities (Saito et al., 2002; Uno
286 et al., 1996), particularly during winter, and such conditions may trap pollutants and alter the NO_x to nitrate
287 photo-oxidation pathway thereby helping facilitate reaction of OH with NO₂ and/or NO with peroxy radicals.

288 Regardless of the precise mechanism driving down $\Delta^{17}\text{O}_{\text{dry}}$ at Sapporo, such low values suggest two
289 distinct sources of nitrate in wet and dry deposition in our study region. The first is likely transported relatively long
290 distances to both Rishiri and Sapporo in wet deposition and to Rishiri in dry deposition. Below-cloud scavenging of
291 local/regional particulate nitrate and gaseous HNO₃ undoubtedly occurs at the beginning of precipitation events, but
292 the similar absolute values and temporal variations of $\Delta^{17}\text{O}_{\text{wet}}$ at both sites suggest that the majority of nitrate in wet
293 deposition at Sapporo (as well as Rishiri) originates from afar and is transported to Japan in cloud water. The second
294 source is likely local anthropogenic NO_x emissions that are deposited in dry deposition near their point of production
295 at the urban site, Sapporo, as concentrations of OH and peroxy radicals are typically elevated in more polluted urban
296 environments (Monks, 2005). Similarly, the more positive values of $\Delta^{17}\text{O}_{\text{coarse}}$ than $\Delta^{17}\text{O}_{\text{fine}}$ at both sites suggest that
297 nitrate in coarse particles is subject to greater supply through long-range transport (produced in free troposphere)
298 than is nitrate in fine particles, which are more influenced by local sources (produced within the boundary layer of
299 the urban area).

300 To aid our interpretations based on $\Delta^{17}\text{O}$ we evaluated $\delta^{15}\text{N}$ values of nitrate, which we interpret as
301 primarily indicating variation in NO_x oxidation efficiency (e.g. Walters and Michalski, 2015, 2016; Walters et al.,
302 2016). We recognize that nitrate $\delta^{15}\text{N}$ values are influenced by factors that are difficult to constrain in our study,
303 including the $\delta^{15}\text{N}$ values of NO_x from the East Asian continent, the removal rate of NO_x (or production rate of

304 nitrate) during transport, isotopic fractionation between NO_x and nitrate during in-cloud and below-cloud
305 scavenging processes during transport, the $\delta^{15}\text{N}$ values of locally produced NO_x , and the relative amount of NO_x
306 derived locally vs. that from the East Asian continent. Nevertheless, the last factor likely differs the most between
307 our sites since there is more locally produced NO_x in the urban environment at Sapporo. During long-distance
308 transport of NO_x there is greater ^{15}N -enrichment in NO_2 than NO (Freyer, 1991), which causes the residual NO_x to
309 become depleted in ^{15}N during partial removal of NO_x as nitrate in the troposphere. Therefore, nitrate derived from
310 long-distance transport from the East Asian continent is likely to have lower $\delta^{15}\text{N}$ values than nitrate from more
311 local sources. The relatively high $\delta^{15}\text{N}_{\text{dry}}$ values at Sapporo are consistent with this interpretation and with the
312 $\Delta^{17}\text{O}$ -based inference that nitrate in dry deposition at Sapporo originates from more local sources than does that in
313 wet deposition at Sapporo and both forms of deposition at Rishiri.

314 The correlations between $\Delta^{17}\text{O}$ and $\delta^{15}\text{N}$ for both forms of deposition at both sites, with the exception of
315 dry deposition at Sapporo, suggest a relationship between oxidation pathways (recorded by $\Delta^{17}\text{O}$) and NO_x oxidation
316 efficiency (recorded by $\delta^{15}\text{N}$). Both NO_x oxidation pathways and efficiencies are primarily controlled by the rate of
317 the $\text{NO}_2 + \text{OH}$ reaction, which suggests that this reaction drives these correlations. The lack of correlation between
318 $\Delta^{17}\text{O}_{\text{dry}}$ and $\delta^{15}\text{N}_{\text{dry}}$ at Sapporo likely reflects the unique oxidation pathways (and thus $\Delta^{17}\text{O}$ values) associated with
319 locally produced NO_x in the urban environment.

320 At both sites, wet and dry deposition exhibited generally larger $\delta^{15}\text{N}$ values in the winter than summer
321 months. This result probably occurs because of seasonal changes in temperature on isotopic fractionation of nitrogen
322 isotopes and/or in the proportion of NO_2 in NO_x (Walters et al., 2016). Overall, our $\delta^{15}\text{N}$ data suggest that nitrate
323 undergoing long-distance transport and/or production during the summer is likely to have experienced higher NO_x
324 oxidation efficiency than that produced locally and/or during the winter. $\delta^{15}\text{N}$ values of nitrate likely only reflect
325 those of the source NO_x for nitrate produced locally during the winter. Indeed, the relatively high $\delta^{15}\text{N}_{\text{dry}}$ values
326 during the winter at Sapporo are consistent with those expected for sources such as nearby combustion of fossil fuels
327 (Redling et al., 2013; Walters et al., 2015).

328 Overall, our results imply that local-scale efforts to reduce nitrate deposition resulting from local NO_x
329 emissions will be most effective to the extent that dry deposition is the dominant form of atmospheric deposition.
330 Local efforts may be less effective in places and times where atmospheric deposition arrives as wet deposition, since
331 wet deposition seems more likely to originate from long distances. Thus, regional, national and global efforts will
332 likely be required to reduce the effects of atmospheric nitrate in wet deposition that is transported long distances in
333 air masses. Additional datasets with paired measurements of $\Delta^{17}\text{O}_{\text{wet}}$ and $\Delta^{17}\text{O}_{\text{dry}}$ would be valuable to evaluate our
334 interpretation of the oxidation pathways and sources and transport distances of nitrate deposited in urban
335 environments.

336 The $\Delta^{17}\text{O}$ values of nitrate are increasingly used in watershed studies to determine the relative abundance of
337 unprocessed atmospheric nitrate in environmental waters, such as rivers and lakes (Sabo et al., 2016; Riha et al.,
338 2015; Tsunogai et al., 2016; Tsunogai et al., 2010; Michalski et al., 2004). Such studies often use $\Delta^{17}\text{O}_{\text{wet}}$ or $\Delta^{17}\text{O}_{\text{dry}}$
339 as an end-member for calculating the amount of unprocessed atmospheric nitrate in a sample. Although they should
340 be validated at other sites, our results suggest that it may be reasonable to assume that $\Delta^{17}\text{O}_{\text{wet}}$ and $\Delta^{17}\text{O}_{\text{dry}}$ are
341 similar in rural settings, since the annual weighted-average $\Delta^{17}\text{O}$ values of wet and dry were nearly identical (+27.2
342 and +27.1 ‰, respectively) at Rishiri. However, in urban settings or settings downstream of urban environments the
343 potential differences between $\Delta^{17}\text{O}_{\text{wet}}$ and $\Delta^{17}\text{O}_{\text{dry}}$ may need to be considered to avoid over- or under-estimating the
344 amount of unprocessed atmospheric nitrate when using $\Delta^{17}\text{O}$ values of nitrate as a tracer of atmospheric nitrate. For
345 example, consider a simple mixing model such as % atmospheric nitrate = $100 \times [(\Delta^{17}\text{O}_{\text{measured}} -$
346 $\Delta^{17}\text{O}_{\text{terrestrial}})/(\Delta^{17}\text{O}_{\text{atmospheric}} - \Delta^{17}\text{O}_{\text{terrestrial}})]$
347 where $\Delta^{17}\text{O}_{\text{measured}}$ is the $\Delta^{17}\text{O}$ value of nitrate in a stream sample, $\Delta^{17}\text{O}_{\text{terrestrial}}$ is the $\Delta^{17}\text{O}$ value of nitrate containing
348 no atmospheric nitrate (i.e., 0 ‰), and $\Delta^{17}\text{O}_{\text{atmospheric}}$ is the $\Delta^{17}\text{O}$ value of atmospheric nitrate (either +27.6 or
349 +21.8 ‰, representing the average weighted-average annual values of $\Delta^{17}\text{O}_{\text{wet}}$ and $\Delta^{17}\text{O}_{\text{dry}}$ measured at Sapporo in
350 the present study). The difference in % atmospheric nitrate when +27.6 vs. +21.8 ‰ are used as end-members for
351 $\Delta^{17}\text{O}_{\text{atmospheric}}$ is small when $\Delta^{17}\text{O}_{\text{measured}}$ is small (e.g. ~1 % when $\Delta^{17}\text{O}_{\text{measured}}$ is ~1 ‰), but increases when

352 $\Delta^{17}\text{O}_{\text{measured}}$ is large (e.g. $\sim 19\%$ when $\Delta^{17}\text{O}_{\text{measured}}$ is 20‰). Thus, our results suggest a weighted average of $\Delta^{17}\text{O}_{\text{wet}}$
353 and $\Delta^{17}\text{O}_{\text{dry}}$ should be used when $\Delta^{17}\text{O}$ values of nitrate are used to quantify the amount of unprocessed atmospheric
354 nitrate exported from urban watersheds. At Sapporo, the weighted average of $\Delta^{17}\text{O}_{\text{wet}}$ and $\Delta^{17}\text{O}_{\text{dry}}$ is $+25.7\text{‰}$, which
355 is more similar to $\Delta^{17}\text{O}_{\text{wet}}$ than $\Delta^{17}\text{O}_{\text{dry}}$ at this site since wet deposition comprised the majority of the total deposition
356 at this site. However, $\Delta^{17}\text{O}_{\text{wet}}$ may not as closely approximate the weighted average of $\Delta^{17}\text{O}_{\text{wet}}$ and $\Delta^{17}\text{O}_{\text{dry}}$ at some
357 sites, such as semi-closed and/or highly polluted urban areas, where the majority of deposition comes from local
358 sources.

359

360 **5 Conclusions**

361 Our isotopic data suggest differences in the oxidation chemistry and transport distances of wet and dry
362 deposition in urban settings: wet deposition tends to originate from afar, whereas dry deposition is produced largely
363 from local sources as the result of unique NO_x oxidation pathways that occur in polluted urban settings. These
364 results imply that reductions in local NO_x emissions will be most effective when and where dry deposition is the
365 dominant form of atmospheric deposition, which has implications for efforts to reduce nitrate deposition and its
366 negative environmental impacts in cities and downwind areas. The approach used herein of comparing isotopic
367 values of wet and dry deposition in different environmental settings is likely to provide continued insight into the
368 transport distances and reaction pathways of atmospheric nitrate pollution.

369 *Data availability.* All data are available upon request from the corresponding author. *Author contributions.* UT, TO,
370 and FN designed the study. UT, TO, DD, FN, IN, TY carried out the research. DMN and DD performed data
371 analysis. DMN and TO wrote the manuscript with contributions from all authors. All authors have given approval to
372 the final version of the manuscript.

373

374 *Competing interests.* The authors declare that they have no conflict of interest.

375

376 *Acknowledgements.* We thank the Ministry of the Environment, Japan, for providing the monitoring data of the acid
377 deposition survey and Joel Bostic for providing feedback on an earlier version of the manuscript. This work was
378 supported by a Grant-in-Aid for Scientific Research from the Ministry of Education, Culture, Sports, Science, and
379 Technology of Japan under grants 26241006 and 17H00780 (to UT and FN), 15H02804 and 15K12187 (to FN), as
380 well as a visiting research fellowship from Nagoya University and short-term invitation fellowship (grant S17093)
381 from Japan Society for Promotion of Science (to DMN).

382

383 **References**

384 Aikawa, M., Ohara, T., Hiraki, T., Oishi, O., Tsuji, A., Yamagami, M., Murano, K., and Mukai, H.: Significant
385 geographic gradients in particulate sulfate over Japan determined from multiple-site measurements and a chemical
386 transport model: Impacts of transboundary pollution from the Asian continent, *Atmos Environ*, 44, 381-391,
387 10.1016/j.atmosenv.2009.10.025, 2010.

388 Akimoto, H.: Global air quality and pollution, *Science*, 302, 1716-1719, DOI 10.1126/science.1092666, 2003.

389 Alexander, B., Hastings, M. G., Allman, D. J., Dachs, J., Thornton, J. A., and Kunasek, S. A.: Quantifying
390 atmospheric nitrate formation pathways based on a global model of the oxygen isotopic composition ($\Delta^{17}\text{O}$) of
391 atmospheric nitrate, *Atmos Chem Phys*, 9, 5043-5056, 2009.

392 Balestrini, R., Galli, L., and Tartari, G.: Wet and dry atmospheric deposition at prealpine and alpine sites in northern
393 Italy, *Atmos Environ*, 34, 1455-1470, Doi 10.1016/S1352-2310(99)00404-5, 2000.

394 Ban, S., Matsuda, K., Sato, K., and Ohizumi, T.: Long-term assessment of nitrogen deposition at remote EANET
395 sites in Japan, *Atmos Environ*, 146, 70-78, 10.1016/j.atmosenv.2016.04.015, 2016.

396 Bloom, D. E., Canning, D., and Fink, G.: Urbanization and the wealth of nations, *Science*, 319, 772-775,
397 10.1126/science.1153057, 2008.

398 Brown, S. S., Ryerson, T. B., Wollny, A. G., Brock, C. A., Peltier, R., Sullivan, A. P., Weber, R. J., Dube, W. P.,
399 Trainer, M., Meagher, J. F., Fehsenfeld, F. C., and Ravishankara, A. R.: Variability in nocturnal nitrogen oxide
400 processing and its role in regional air quality, *Science*, 311, 67-70, 10.1126/science.1120120, 2006.

401 Carslaw, N., Creasey, D. J., Heard, D. E., Jacobs, P. J., Lee, J. D., Lewis, A. C., McQuaid, J. B., Pilling, M. J.,
402 Bauguitte, S., Penkett, S. A., Monks, P. S., and Salisbury, G.: Eastern Atlantic Spring Experiment 1997 (EASE97) -
403 2. Comparisons of model concentrations of OH, HO₂, and RO₂ with measurements, *J Geophys Res-Atmos*, 107,
404 Artn 4190
405 10.1029/2001jd001568, 2002.

406 Casciotti, K. L., Bohlke, J. K., McIlvin, M. R., Mroczkowski, S. J., and Hannon, J. E.: Oxygen isotopes in nitrite:
407 Analysis, calibration, and equilibration, *Anal Chem*, 79, 2427-2436, 10.1021/ac061598h, 2007.

408 Celle-Jeanton, H., Travi, Y., Loye-Pilot, M. D., Huneau, F., and Bertrand, G.: Rainwater chemistry at a
409 Mediterranean inland station (Avignon, France): Local contribution versus long-range supply, *Atmos Res*, 91,
410 118-126, 10.1016/j.atmosres.2008.06.003, 2009.

411 Crutzen, P. J.: Role of NO and NO₂ in the chemistry of the troposphere and stratosphere, *Annu Rev Earth Pl Sc*, 7,
412 443-472, DOI 10.1146/annurev.ea.07.050179.002303, 1979.

413 Cumming, G. S., Buerkert, A., Hoffmann, E. M., Schlecht, E., von Cramon-Taubadel, S., and Tschardtke, T.:
414 Implications of agricultural transitions and urbanization for ecosystem services, *Nature*, 515, 50-57,
415 10.1038/nature13945, 2014.

416 Dasch, J. M., and Cadle, S. H.: Wet and dry deposition monitoring in southeastern Michigan, *Atmos Environ*, 19,
417 789-796, Doi 10.1016/0004-6981(85)90067-8, 1985.

418 Elliott, E. M., Kendall, C., Boyer, E. W., Burns, D. A., Lear, G. G., Golden, H. E., Harlin, K., Bytnerowicz, A.,
419 Butler, T. J., and Glatz, R.: Dual nitrate isotopes in dry deposition: Utility for partitioning NO_x source contributions
420 to landscape nitrogen deposition, *J Geophys Res-Bioge*, 114, -, 2009.

421 Endo, T., Yagoh, H., Sato, K., Matsuda, K., Hayashi, K., Noguchi, I., and Sawada, K.: Regional characteristics of
422 dry deposition of sulfur and nitrogen compounds at EANET sites in Japan from 2003 to 2008, *Atmos Environ*, 45,
423 1259-1267, 10.1016/j.atmosenv.2010.12.003, 2011.

424 Erisman, J. W., Draaijers, G., Duyzer, J., Hofschreuder, P., VanLeeuwen, N., Romer, F., Ruijgrok, W., Wyers, P.,
425 and Gallagher, M.: Particle deposition to forests - Summary of results and application, *Atmos Environ*, 31, 321-332,
426 Doi 10.1016/S1352-2310(96)00223-3, 1997.

427 Fang, Y. T., Koba, K., Wang, X. M., Wen, D. Z., Li, J., Takebayashi, Y., Liu, X. Y., and Yoh, M.: Anthropogenic
428 imprints on nitrogen and oxygen isotopic composition of precipitation nitrate in a nitrogen-polluted city in southern
429 China, *Atmos Chem Phys*, 11, 1313-1325, 10.5194/acp-11-1313-2011, 2011.

430 Fraser, M. P., Cass, G. R., and Simoneit, B. R. T.: Gas-phase and particle-phase organic compounds emitted from
431 motor vehicle traffic in a Los Angeles roadway tunnel, *Environ Sci Technol*, 32, 2051-2060, DOI
432 10.1021/es970916e, 1998.

433 Freyer, H. D.: Seasonal variation of ¹⁵N/¹⁴N ratios in atmospheric nitrate species, *Tellus B*, 43, 30-44, DOI
434 10.1034/j.1600-0889.1991.00003.x, 1991.

435 Freyer, H. D., Kley, D., Volzthomas, A., and Kobel, K.: On the interaction of isotopic exchange processes with
436 photochemical reactions in atmospheric oxides of nitrogen, *J Geophys Res-Atmos*, 98, 14791-14796, Doi
437 10.1029/93jd00874, 1993.

438 Galloway, J. N., Dentener, F. J., Capone, D. G., Boyer, E. W., Howarth, R. W., Seitzinger, S. P., Asner, G. P.,
439 Cleveland, C. C., Green, P. A., Holland, E. A., Karl, D. M., Michaels, A. F., Porter, J. H., Townsend, A. R., and
440 Vorosmarty, C. J.: Nitrogen cycles: past, present, and future, *Biogeochemistry*, 70, 153-226, 2004.

441 Geng, L., Murray, L. T., Mickley, L. J., Lin, P., Fu, Q., Schauer, A. J., and Alexander, B.: Isotopic evidence of

442 multiple controls on atmospheric oxidants over climate transitions, *Nature*, 546, 133-+, 10.1038/nature22340, 2017.

443 Guerrieri, R., Vanguelova, E. I., Michalski, G., Heaton, T. H. E., and Mencuccini, M.: Isotopic evidence for the
444 occurrence of biological nitrification and nitrogen deposition processing in forest canopies, *Glob Change Biol*, 21,
445 4613-4626, 10.1111/gcb.13018, 2015.

446 Guha, T., Lin, C. T., Bhattacharya, S. K., Mahajan, A. S., Ou-Yang, C.-F., Lan, Y.-P., Hsu, S. C., and Liang, M.-C.:
447 Isotopic ratios of nitrate in aerosol samples from Mt. Lulin, a high-altitude station in Central Taiwan, *Atmos*
448 *Environ*, 154, 53-69, 2017.

449 Gurjar, B. R., Ravindra, K., and Nagpure, A. S.: Air pollution trends over Indian megacities and their local-to-global
450 implications, *Atmos Environ*, 142, 475-495, 10.1016/j.atmosenv.2016.06.030, 2016.

451 Hammer, Ø., Harper, D. A. T., and Ryan, P. D.: PAST: Paleontological statistics software package for education and
452 data analysis, *Palaeontologia Electronica*, 4, 9, 2001.

453 Hicks, B. B.: Measuring dry deposition: A reassessment of the state-of-the-art, *Water Air Soil Poll*, 30, 75-90, Doi
454 10.1007/Bf00305177, 1986.

455 Hirota, A., Tsunogai, U., Komatsu, D. D., and Nakagawa, F.: Simultaneous determination of $\delta^{15}\text{N}$ and $\delta^{18}\text{O}$ of N_2O
456 and $\delta^{13}\text{C}$ of CH_4 in nanomolar quantities from a single water sample, *Rapid Commun Mass Sp*, 24, 1085-1092,
457 10.1002/rcm.4483, 2010.

458 Holtgrieve, G. W., Schindler, D. E., Hobbs, W. O., Leavitt, P. R., Ward, E. J., Bunting, L., Chen, G. J., Finney, B. P.,
459 Gregory-Eaves, I., Holmgren, S., Lisac, M. J., Lisi, P. J., Nydick, K., Rogers, L. A., Saros, J. E., Selbie, D. T.,
460 Shapley, M. D., Walsh, P. B., and Wolfe, A. P.: A coherent signature of anthropogenic nitrogen deposition to remote
461 watersheds of the Northern hemisphere, *Science*, 334, 1545-1548, 2011.

462 Kaiser, J., Hastings, M. G., Houlton, B. Z., Rockmann, T., and Sigman, D. M.: Triple oxygen isotope analysis of
463 nitrate using the denitrifier method and thermal decomposition of N_2O , *Anal Chem*, 79, 599-607, 2007.

464 Kaneyasu, N., Ohta, S., and Muraio, N.: Seasonal variation in the chemical composition of atmospheric aerosols and
465 gaseous species in Sapporo, Japan, *Atmos Environ*, 29, 1559-1568, Doi 10.1016/1352-2310(94)00356-P, 1995.

466 Kendall, C., Elliott, E. M., and Wankel, S. D.: Tracing anthropogenic input of nitrogen to ecosystems, in: *Stable*
467 *Isotopes in Ecology and Environmental Science*, edited by: Michener, R. H., and Lajtha, L. J., Blackwell, Oxford,
468 2007.

469 Komatsu, D. D., Ishimura, T., Nakagawa, F., and Tsunogai, U.: Determination of the $^{15}\text{N}/^{14}\text{N}$, $^{17}\text{O}/^{16}\text{O}$, and $^{18}\text{O}/^{16}\text{O}$
470 ratios of nitrous oxide by using continuous-flow isotope-ratio mass spectrometry, *Rapid Commun Mass Sp*, 22,
471 1587-1596, 2008.

472 Li, Y., Schichtel, B. A., Walker, J. T., Schwede, D. B., Chen, X., Lehmann, C. M. B., Puchalski, M. A., Gay, D. A.,
473 and Collett, J. L.: Increasing importance of deposition of reduced nitrogen in the United States, *P Natl Acad Sci*
474 *USA*, 113, 5874-5879, 10.1073/pnas.1525736113, 2016.

475 Lin, M. Y., Horowitz, L. W., Payton, R., Fiore, A. M., and Tonnesen, G.: US surface ozone trends and extremes
476 from 1980 to 2014: Quantifying the roles of rising Asian emissions, domestic controls, wildfires, and climate,
477 *Atmos Chem Phys*, 17, 2943-2970, 10.5194/acp-17-2943-2017, 2017.

478 Liu, F., Zhang, Q., Ronald, J. V., Zheng, B., Tong, D., Yan, L., Zheng, Y. X., and He, K. B.: Recent reduction in
479 NO_x emissions over China: synthesis of satellite observations and emission inventories, *Environ Res Lett*, 11, Artn
480 114002
481 10.1088/1748-9326/11/11/114002, 2016.

482 McIlvin, M. R., and Altabet, M. A.: Chemical conversion of nitrate and nitrite to nitrous oxide for nitrogen and
483 oxygen isotopic analysis in freshwater and seawater, *Anal Chem*, 77, 5589-5595, 10.1021/ac050528s, 2005.

484 Mehlmann, A., and Warneck, P.: Atmospheric gaseous HNO₃, particulate nitrate, and aerosol-size distributions of
485 major ionic species at a rural site in western Germany, *Atmos Environ*, 29, 2359-2373, Doi
486 10.1016/1352-2310(95)00056-5, 1995.

487 Michalski, G., Scott, Z., Kabling, M., and Thiemens, M. H.: First measurements and modeling of $\Delta^{17}\text{O}$ in
488 atmospheric nitrate, *Geophys Res Lett*, 30, 2003.

489 Michalski, G., Meixner, T., Fenn, M., Hernandez, L., Sirulnik, A., Allen, E., and Thiemens, M.: Tracing
490 atmospheric nitrate deposition in a complex semiarid ecosystem using $\Delta^{17}\text{O}$, *Environ Sci Technol*, 38, 2175-2181,
491 2004.

492 Michalski, G., Bhattacharya, S. K., and Mase, D. F.: Oxygen Isotope Dynamics of Atmospheric Nitrate and Its
493 Precursor Molecules, in: *Handbook of Environmental Isotope Geochemistry, Advances in Isotope Geochemistry*,
494 edited by: Baskaran, M., Springer Verlag, Berlin, 613-635, 2011.

495 Monks, P. S.: Gas-phase radical chemistry in the troposphere, *Chem Soc Rev*, 34, 376-395, 10.1039/b307982c,
496 2005.

497 Morin, S., Savarino, J., Frey, M. M., Yan, N., Bekki, S., Bottenheim, J. W., and Martins, J. M. F.: Tracing the origin
498 and fate of NO_x in the Arctic atmosphere using stable isotopes in nitrate, *Science*, 322, 730-732,
499 10.1126/science.1161910, 2008.

500 Morin, S., Sander, R., and Savarino, J.: Simulation of the diurnal variations of the oxygen isotope anomaly (Δ
501 O-17) of reactive atmospheric species, *Atmos Chem Phys*, 11, 3653-3671, 10.5194/acp-11-3653-2011, 2011.

502 Nations, U.: *World Urbanization Prospects, the 2014 Revision*, United Nations, Population Division, Department of
503 Economic and Social Affairs, New York, 2014.

504 Noguchi, I., Aoi, B., Takada, M., Hamahara, K., Takahashi, H., and Tamada, K.: Developing NDVI Estimation
505 Model of Forest Area in Japan, using Temperature data, *Report of Institute of Environmental Sciences*, 43-56, 2006.

506 Noguchi, I., Yamaguchi, T., Sakai, S., and Tsunogai, U.: Comparison of air pollutant measurements by weekly,
507 biweekly, and monthly filter-pack method, *Proceedings of the 50th Annual meeting of Japan Society for*
508 *Atmospheric Environment*, 2009.

509 Noguchi, I., Yamaguchi, T., Kawamura, M., Matsumoto, R., and Matsuda, K.: Updated program file for dry
510 deposition velocity, *Report of Institute of Environmental Sciences*, 21-31, 2011.

511 Redling, K., Elliott, E., Bain, D., and Sherwell, J.: Highway contributions to reactive nitrogen deposition: tracing the
512 fate of vehicular NO_x using stable isotopes and plant biomonitors, *Biogeochemistry*, 116, 261-274,
513 10.1007/s10533-013-9857-x, 2013.

514 Riha, K. M., Michalski, G., Gallo, E. L., Lohse, K. A., Brooks, P. D., and Meixner, T.: High atmospheric nitrate
515 inputs and nitrogen turnover in semi-arid urban catchments, *Ecosystems*, 17, 1309–1325, 2015.

516 Sabo, R. D., Nelson, D. M., and Eshleman, K. N.: Episodic, seasonal, and annual export of atmospheric and
517 microbial nitrate from a temperate forest, *Geophys Res Lett*, 43, 683-691, 10.1002/2015gl066758, 2016.

518 Saito, S., Nagao, I., and Tanaka, H.: Relationship of NO_x and NMHC to photochemical O₃ production in a coastal
519 and metropolitan areas of Japan, *Atmos Environ*, 36, 1277-1286, Pii S1352-2310(01)00557-X
520 Doi 10.1016/S1352-2310(01)00557-X, 2002.

521 Savarino, J., Kaiser, J., Morin, S., Sigman, D. M., and Thiemens, M. H.: Nitrogen and oxygen isotopic constraints
522 on the origin of atmospheric nitrate in coastal Antarctica, *Atmos Chem Phys*, 7, 1925-1945, 2007.

523 Skyllakou, K., Murphy, B. N., Megaritis, A. G., Fountoukis, C., and Pandis, S. N.: Contributions of local and
524 regional sources to fine PM in the megacity of Paris, *Atmos Chem Phys*, 14, 2343-2352, 10.5194/acp-14-2343-2014,
525 2014.

526 Sofen, E. D., Alexander, B., Steig, E. J., Thiemens, M. H., Kunasek, S. A., Amos, H. M., Schauer, A. J., Hastings,
527 M. G., Bautista, J., Jackson, T. L., Vogel, L. E., McConnell, J. R., Pasteris, D. R., and Saltzman, E. S.: WAIS Divide
528 ice core suggests sustained changes in the atmospheric formation pathways of sulfate and nitrate since the 19th
529 century in the extratropical Southern Hemisphere, *Atmos Chem Phys*, 14, 5749-5769, 10.5194/acp-14-5749-2014,
530 2014.

531 Tørseth, K., Hanssen, J. E., and Semb, A.: Temporal and spatial variations of airborne Mg, Cl, Na, Ca and K in rural
532 areas of Norway, *Sci Total Environ*, 234, 75-85, Doi 10.1016/S0048-9697(99)00261-2, 1999.

533 Tsunogai, U., Kido, T., Hirota, A., Ohkubo, S. B., Komatsu, D. D., and Nakagawa, F.: Sensitive determinations of
534 stable nitrogen isotopic composition of organic nitrogen through chemical conversion into N₂O, *Rapid Commun*
535 *Mass Sp*, 22, 345-354, 10.1002/rcm.3368, 2008.

536 Tsunogai, U., Komatsu, D. D., Daita, S., Kazemi, G. A., Nakagawa, F., Noguchi, I., and Zhang, J.: Tracing the fate
537 of atmospheric nitrate deposited onto a forest ecosystem in Eastern Asia using $\Delta^{17}\text{O}$, *Atmos Chem Phys*, 10,
538 1809-1820, 2010.

539 Tsunogai, U., Miyauchi, T., Ohyama, T., Komatsu, D. D., Nakagawa, F., Obata, Y., Sato, K., and Ohizumi, T.:
540 Accurate and precise quantification of atmospheric nitrate in streams draining land of various uses by using triple
541 oxygen isotopes as tracers, *Biogeosciences*, 13, 3441-3459, 10.5194/bg-13-3441-2016, 2016.

542 Uno, I., Wakamatsu, S., and Ueda, H.: Behavior of nocturnal urban boundary layer and air pollutants, *Journal of*
543 *Japan Society of Air Pollution*, 23, 102-114, 1988.

544 Uno, I., Ohara, T., and Wakamatsu, S.: Analysis of wintertime NO₂ pollution in the Tokyo Metropolitan area,
545 *Atmos Environ*, 30, 703-713, Doi 10.1016/1352-2310(95)00177-8, 1996.

546 Uno, I., Uematsu, M., Hara, Y., He, Y. J., Ohara, T., Mori, A., Kamaya, T., Murano, K., Sadanaga, Y., and Bandow,
547 H.: Numerical study of the atmospheric input of anthropogenic total nitrate to the marginal seas in the western North
548 Pacific region, *Geophys Res Lett*, 34, Artn L17817
549 10.1029/2007gl030338, 2007.

550 von Glasow, R., Jickells, T. D., Baklanov, A., Carmichael, G. R., Church, T. M., Gallardo, L., Hughes, C.,
551 Kanakidou, M., Liss, P. S., Mee, L., Raine, R., Ramachandran, P., Ramesh, R., Sundseth, K., Tsunogai, U., Uematsu,
552 M., and Zhu, T.: Megacities and large urban agglomerations in the coastal zone: Interactions between atmosphere,
553 land, and marine ecosystems, *Ambio*, 42, 13-28, 10.1007/s13280-012-0343-9, 2013.

554 Wagstrom, K. M., and Pandis, S. N.: Contribution of long range transport to local fine particulate matter concerns,
555 *Atmos Environ*, 45, 2730-2735, 10.1016/j.atmosenv.2011.02.040, 2011.

556 Walcek, C. J., Brost, R. A., Chang, J. S., and Wesely, M. L.: SO₂, sulfate and HNO₃ deposition velocities computed
557 using regional landuse and meteorological data, *Atmos Environ*, 20, 949-964, Doi 10.1016/0004-6981(86)90279-9,
558 1986.

559 Walters, W. W., and Michalski, G.: Theoretical calculation of nitrogen isotope equilibrium exchange fractionation
560 factors for various NO_y molecules, *Geochim Cosmochim Acta*, 164, 284-297, 10.1016/j.gca.2015.05.029, 2015.

561 Walters, W. W., Tharp, B. D., Fang, H., Kozak, B. J., and Michalski, G.: Nitrogen isotope composition of thermally
562 produced NO_x from various fossil-fuel combustion sources, *Environ Sci Technol*, 49, 11363-11371,
563 10.1021/acs.est.5b02769, 2015.

564 Walters, W. W., and Michalski, G.: Theoretical calculation of oxygen equilibrium isotope fractionation factors
565 involving various NO_y molecules, OH, and H₂O and its implications for isotope variations in atmospheric nitrate,
566 *Geochim Cosmochim Acta*, 191, 89-101, 10.1016/j.gca.2016.06.039, 2016.

567 Walters, W. W., Simonini, D. S., and Michalski, G.: Nitrogen isotope exchange between NO and NO₂ and its
568 implications for δ¹⁵N variations in tropospheric NO_x and atmospheric nitrate, *Geophys Res Lett*, 43, 440-448,
569 10.1002/2015gl066438, 2016.

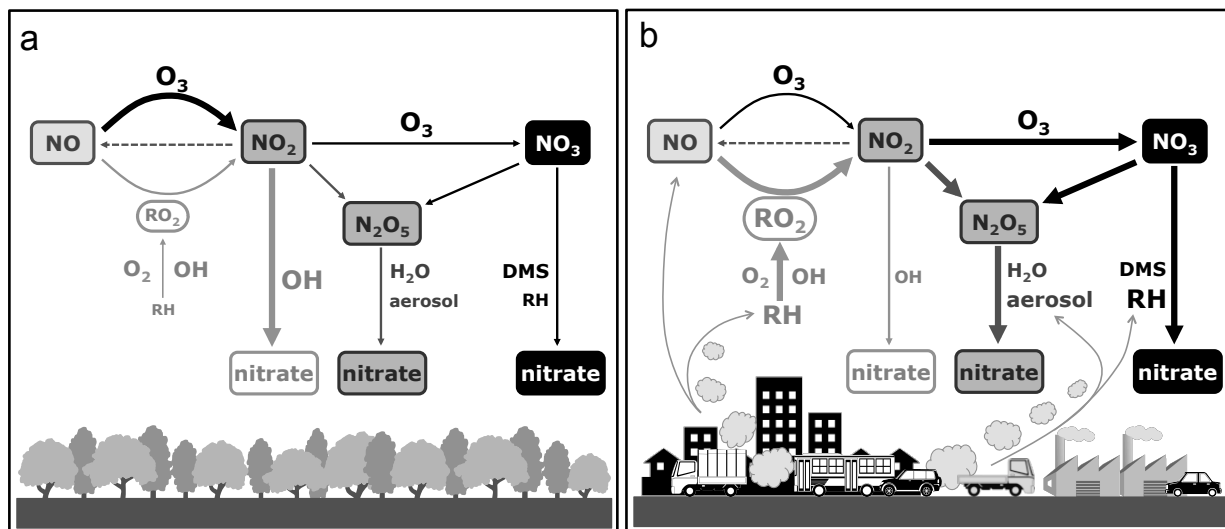
570 Wesely, M. L.: Parameterization of surface resistances to gaseous dry deposition in regional-scale numerical models,
571 *Atmos Environ*, 23, 1293-1304, Doi 10.1016/0004-6981(89)90153-4, 1989.

572 Zhang, L., Brook, J. R., and Vet, R.: A revised parameterization for gaseous dry deposition in air-quality models,
573 *Atmos Chem Phys*, 3, 2067-2082, 2003.

574 Zhao, Y., Qiu, L. P., Xu, R. Y., Xie, F. J., Zhang, Q., Yu, Y. Y., Nielsen, C. P., Qin, H. X., Wang, H. K., Wu, X. C.,
575 Li, W. Q., and Zhang, J.: Advantages of a city-scale emission inventory for urban air quality research and policy:
576 The case of Nanjing, a typical industrial city in the Yangtze River Delta, China, *Atmos Chem Phys*, 15,
577 12623-12644, 10.5194/acp-15-12623-2015, 2015.

578
579
580
581
582
583
584
585

586



587

588 **Figure 1.** Conceptual diagrams of pathways for conversion of NO_x (NO + NO₂) to nitrate (NO₃⁻) in a) background
589 atmosphere and b) urban atmosphere. The first step in the process is the conversion of NO to NO₂, which is
590 accomplished primarily by O₃ or peroxy radicals (HO₂ + RO₂). The second step is the oxidation of NO₂. In daylight
591 OH oxidizes NO₂ to nitrate and at night O₃ oxidizes NO₂ to nitrate. Reactions with dimethylsulfide (DMS) or
592 reactive hydrocarbons (RH) or NO₂ (to form N₂O₅, followed by hydrolysis on aerosol surfaces) provide a pathway
593 for nitrate deposition. Thicker arrows and larger fonts suggest greater relative importance of different pathways
594 between panels on an annual basis. These diagrams are oversimplifications and the arrow and font sizes are
595 qualitative. Furthermore, these diagrams ignore potential seasonal variation, such as the N₂O₅ pathway being
596 relatively more important in rural environments during the winter than summer and the OH pathway being relatively
597 more important in urban environments during the summer than winter.

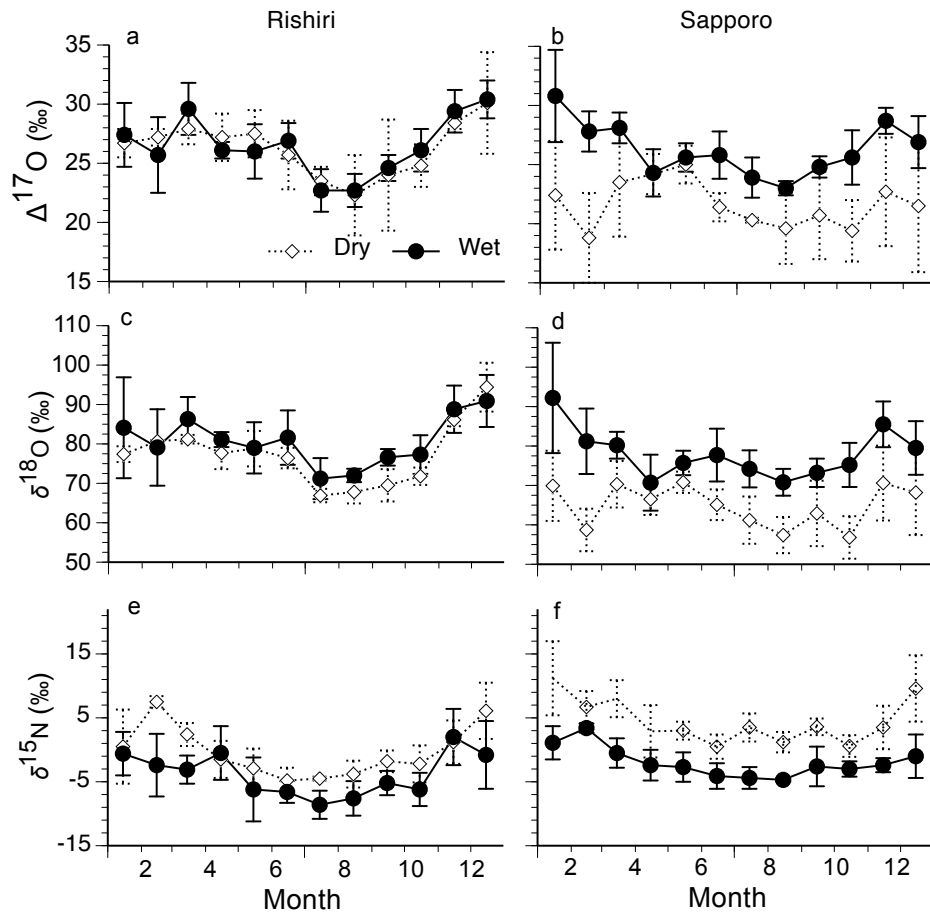
598

599

600

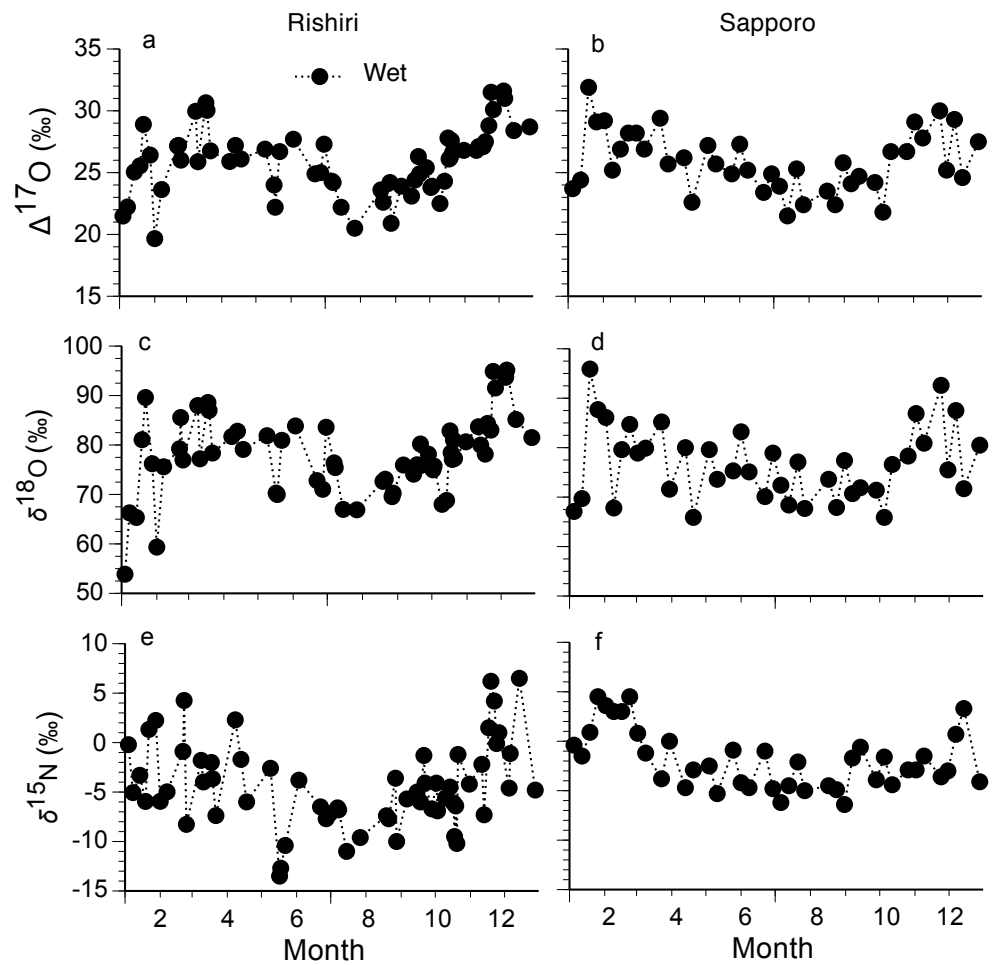
601

602



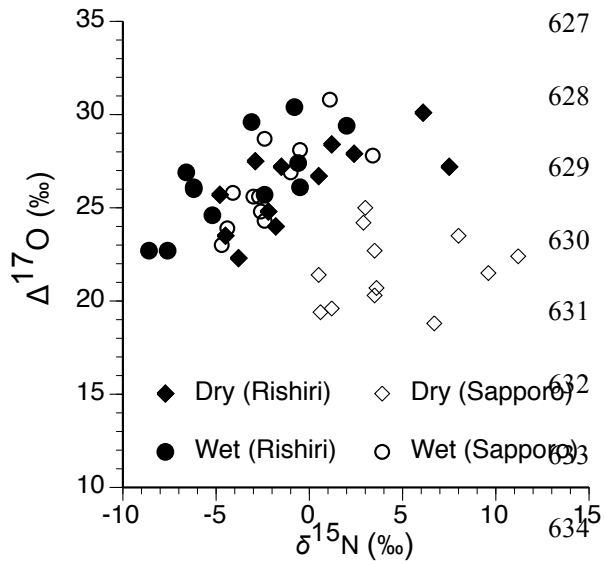
610

611 **Figure 3.** Time series of monthly weighted-average a, b) $\Delta^{17}\text{O}$ values of nitrate in dry and wet deposition c, d) $\delta^{18}\text{O}$
 612 values of nitrate in dry and wet deposition, and e, f) $\delta^{15}\text{N}$ values of nitrate in wet deposition. Data from Rishiri
 613 (rural) are in left column and data from Sapporo (urban) are in right column. Error bars on isotopic values of nitrate
 614 in dry deposition represent one standard deviation of isotopic values of nitrate in coarse and fine particles and in
 615 gaseous form, whereas errors bars on isotopic values of nitrate in wet deposition represent one standard deviation of
 616 all isotopic values of nitrate in wet deposition made during the sampling period.



617
 618 **Figure 4.** Time series of a, b) $\Delta^{17}\text{O}$ values of nitrate in wet deposition, c, d) $\delta^{18}\text{O}$ values of nitrate in wet deposition,
 619 and e, f) $\delta^{15}\text{N}$ values of nitrate in wet deposition. Data from Rishiri (rural) are in left column and data from Sapporo
 620 (urban) are in right column.

621
 622
 623
 624
 625
 626



627
 628
 629
 630
 631
 632
 633
 634
 635

636 **Figure 5.** Correlation of $\delta^{15}\text{N}$ and $\Delta^{17}\text{O}$ values of nitrate in wet and dry deposition at Rishiri and Sapporo. Dry
 637 deposition at Rishiri: slope = 0.57 (95% confidence interval = 0.15 – 0.79), $r = 0.70$, $p = 0.01$, $n = 12$; Wet
 638 deposition at Rishiri: slope = 0.74 (95% confidence interval = 0.43 – 0.97), $r = 0.73$, $p = 0.007$, $n = 12$; Dry
 639 deposition at Sapporo: $r = 0.17$, $p = 0.59$, $n = 12$; Wet deposition at Sapporo: slope = 0.95 (95% confidence interval
 640 = 0.33 – 1.35), $r = 0.73$, $p = 0.007$, $n = 12$.